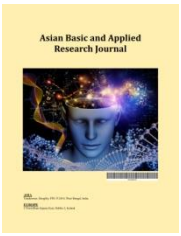

Asian Basic and Applied Research Journal

Volume 6, Issue 1, Page 1-19, 2024; Article no.ABAARJ.1475

Investigation of Ionospheric Irregularities over Nigeria Using the Global Navigation Satellite System

C. C. Onuchukwu [a*] and C. P. Okonkwo [a,b]

[a] Department of Industrial Physics, Chukwuemeka Odumegwu Ojukwu University, Anambra State, Nigeria.
[b] Department of Physics, School of Sciences, Nwafor Orizu College of Education, Nzugbe, Anambra State, Nigeria.

Authors' contributions

This work was carried out in collaboration between both authors. Both authors read and approved the final manuscript.

Article Information

Open Peer Review History:
This journal follows the Advanced Open Peer Review policy. Identity of the Reviewers, Editor(s) and additional Reviewers, peer review comments, different versions of the manuscript, comments of the editors, etc are available here: https://prh.globalpresshub.com/review-history/1475

Original Research Article

Received: 25/11/2023
Accepted: 30/01/2024
Published: 01/02/2024

ABSTRACT

We investigated the occurrence of ionospheric irregularities using the Global Navigation Satellite System (GNSS) total electron content (TEC) and rate of change index (ROTI) over Nigeria during the period of 2011 - 2016. The data was obtained from the fourteen stations of Nigerian permanent GNSS Network (NIGNET, www.nignet.net). MATLAB and GOPI GPS-TEC analysis application software version 2.9.2 was used to extract vertical total electron content (VTEC), time, azimuth and elevation angles, latitudes and longitudes from the raw GPS data. The elevation cut - off mask of 45° was used to reduce multipath error. The irregularities were quantified using the 30 s rate of change total electron content (ROT) and 5 min rate of ROTI, which detect irregularities with scale sizes in the range of 400 m - 2.5 km. The ROTI threshold for an ionospheric irregularity to have occurred was set at ≥ 0.4. The percentage occurrence of ionospheric irregularity varies throughout the periods under study, with March and September equinoxes having the highest occurrence of ionospheric irregularities. We also observed that ionospheric irregularities mostly occur during the night-time in the March and September equinoxes in the year 2014 because of high solar activity.

**Corresponding author: Email: onuchukwu71chika@gmail.com;*

These study on the variations of the ionospheric percentage occurrence and intensities of ionospheric irregularities (characterized by the mean ROTI values) in the African equatorial region can be important in the interpreting and monitoring GNSS ionospheric irregularity occurrence over the stations.

Keywords: Global navigation satellite system (GNSS); total electron content (TEC); ionospheric irregularities; ROT.

1. INTRODUCTION

Ionospheric irregularities are disturbances in the ionosphere which affect propagation of radio waves between space and ground-based systems. They disrupt the transmission of satellite-based radio communication signals, and sometimes cause blackouts of the signals for satellite navigation systems like the Global Positioning system (GPS. Interestingly, these satellite navigation systems have provided avenue to investigate the structure of the ionosphere and the associated irregularities.

“The ionosphere acts as a dispersive medium, slowing GPS radio signals as they travel from GPS satellites to Earth. Irregularities in ionospheric electron density cause variations in refraction and absorption of the signals” [1,2,3]. “Due to the irregularities, the Global Navigation Satellite System (GNSS GPS) signal is drastically changed. These changes give rise to what is called ionospheric scintillation. Ionospheric irregularities are formed at the bottom of the F region of the ionosphere due to the Rayleigh-Taylor gravitational instability mechanics” [1,3,4,5].

The ionospheric irregularities can cause the radio wave signals, with a very high frequency (30-1500 MHz), to have temporal fluctuation in its phase and amplitude. This is evident at the polar regions (where the fluctuations may be moderate), the low-latitude (where the fluctuations may be strong), and the equatorial region (where the fluctuations may be intense), [6,7,8]. These fluctuations depend on the seasonal, diurnal, and height variations, its sampling rate, the solar activity, and the solar cycle [9]. “The GPS which operates using radio waves from satellite is sensitive to ionospheric changes due to geomagnetic storms and signals transmitted for communication and navigation purposes must pass through the ionosphere. Ionospheric irregularities are most common at equatorial latitudes and can have a major impact on system performance and reliability, and commercial satellite designers need to account for these effects. Two propagation effects that are prominent are - range error due to delay of the signal in travelling through the ionosphere, and phase and amplitude scintillation caused by irregularities in electron density distribution and total electron content (TEC)” [10].

The occurrences of ionospheric irregularities can induce pseudo-magnetic anomaly, leading to abnormal/false measurements in some instruments and conditions that are geomagnetic dependent. For instance, flow metering may be affected, automatic corrosion control systems may be maladjusted leading to increase corrosion, field waves along the transmission lines can be affected etc. Hence, there is great need to investigate and understand the pattern of electron density variations at all sites as this will aid in the interpretation of magnetic data used in exploration [11].

Various articles on ionospheric irregularities have indicated that ionospheric irregularities which occur around the equatorial region are observed after sunset [4,12–16].

The frequency of occurrence of ionospheric irregularities, the local time, seasonal, latitude, longitude and the solar activities dependence have been studied by various authors [see e.g.,14,17–28]. We point out these authors that have studied ionospheric irregularities in African region, that most of the studies on ionospheric irregularities largely consider data only during the geomagnetic storms and specific solar activity conditions. These authors used different sampling techniques and time interval to qualitatively and quantitatively studied occurrences and rate of occurrences of ionospheric irregularities over different regions.

“The aim of this study is to investigate the occurrence characteristics of the ionospheric irregularities in Nigeria. We employ data from ground-based GPS receivers at different longitudes under similar condition. This strategy can improve our current understanding on the physical mechanisms responsible for the development and evolution of ionospheric irregularities in the sector, it can provide a more comprehensive picture of the spatial and

temporal variations in ionospheric irregularities" [29]. "Furthermore, this can help identify and differentiate between the various physical mechanisms responsible for the development of ionospheric irregularities can help improve the accuracy of models used for GNSS positioning and navigation by providing a more precise characterization of ionospheric irregularities" [29].

In this study, the GNSS data was obtained from the Nigeria Permanent GNSS Network (NIGNET, www.nignet.net) in the years 2011- 2016. Specifically, we which to obtain the available TEC measurements across Nigeria during the years 2011 -2016. The 30-s ROT (Rate of change of TEC) and 5-min ROTI (Rate of change of TEC Index) values were computed to determine the occurrence or otherwise of ionospheric irregularities at the various stations for each day of year 2011-2016. From the analysis of ROTI, we determine which of the stations in Nigeria, exhibit greater intensity of the irregularities as measured using the ROTI parameter. Analysis of the results of occurrences of ionospheric irregularities at different locations, enabled us to offers plausible explanations to the factors that may be responsible for the observed differences in irregularity intensities at the various stations in Nigeria. Fig. 1 shows the map of the stations that was used in this study and Table 1 indicates the names and the codes of the stations with their elevation above sea level, geographical and magnetic coordinates.

The theory of the Rate of change of TEC (ROT) and the Rate of change of TEC Index (ROTI) that were used for studying the occurrence of irregularities in the ionosphere are well described in [29,30,31,32 and the references there in]. The basic principle harnessed in deriving ionospheric TEC values from GNSS observations is that GNSS signals having different frequencies, experience different ionospheric time delays when they transverse the same portion of the ionosphere. The amount of time delay, t which a GNSS signal of frequency, f will experience in ionospheric time delay t as in equation 1 as

Table 1. List of NIGNET GPS stations

Station Code	City	State	Days of Available Data	Elevation (M)	Geographic		Geomagnetic	
					LAT (N)	LONG (E)	LAT (N)	LONG (E)
ABUZ	Zaria	Kaduna	1313	706.1	11.15	7.64	-0.13	79.95
BKFP	Birni	Kebbi	1597	251.0	12.46	4.22	0.63	76.62
CGGT	Toro	Bauchi	510	917.4	10.12	9.11	-0.78	81.10
CLBR	Calabar	Cross-River	1439	61.5	4.95	8.35	-4.29	80.09
FPNO	Owerri	Imo	214	92.6	5.43	7.03	-3.89	70.85
FUTA	Akure	Ondo	181	416.0	7.30	5.14	-2.58	77.16
FUTY	Yola	Adamawa	1764	248.4	9.34	12.49	-1.28	84.31
GEMB	Gembu	Taraba	154	1348.0	6.92	11.78	-3.00	82.95
HUKP	Katsina	Katsina	738	566.0	12.92	7.59	-1.50	79.77
MDGR	Maiduguri	Borno	280	351.8	11.83	13.13	0.49	84.03
OSGF	Abuja	FCT	1052	533.6	9.02	7.48	-1.51	79.49
RUST	Port-Harcourt	Rivers	303	46.6	4.80	6.97	-4.33	78.75
ULAG	Lagos	Lagos	690	45.5	6.51	3.39	-3.03	75.45
UNEC	Enugu	Enugu	907	255.4	6.42	7.50	-3.23	79.37

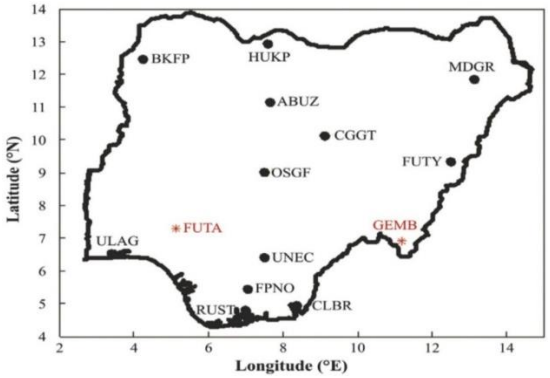

Fig. 1. Geographical map of the GPS stations, (Generated with Matlab)

$$t = 40.3\frac{TEC}{cf^2} \quad (1)$$

where c is the speed of light in free space. f_1 and f_2 are dual frequency of a receiver (receiving the satellite signals at two frequencies,) which measures the difference in time delay between the two frequencies as;

$$\Delta t = t_2 - t_1 = \frac{1}{f_2} - \frac{1}{f_1} \quad (2)$$

t_1 and t_2 are respectively the time delays experienced by the signals of frequencies f_1 and f_2 . The TEC is therefore computed from equations 1 and 2 as shown in equation 3

$$TEC = \frac{c\Delta t}{40.3\left(\frac{1}{f_2^2} - \frac{1}{f_1^2}\right)} \quad (3)$$

To compute TEC values, first, computed vertical total electron content (VTEC) before computing the slant total electron content (STEC). The slant TEC from the pseudo-range measurement is given by [21]

$$STEC = \frac{1}{40.3}\left(\frac{1}{f_2^2} - \frac{1}{f_1^2}\right)(P_1 - P_2) \quad (4)$$

where, P_1 and P_2 are the two Pseudo-ranges in meters measured in two frequencies f_1 and f_2 respectively. Similarly, the slant TEC from carrier phase measurement can be given as [21,30]

$$STEC\ \Phi = \frac{1}{40.3}\left(\frac{1}{f_2^2} - \frac{1}{f_1^2}\right)(\Phi_1 - \Phi_2) \quad (5)$$

where Φ_1 and Φ_2 are phase measurements. The calculation of STEC Φ from pseudo-range observable is absolute but noisy and therefore imprecise, whereas the measure of relative from phase observable is very precise but it is ambiguous because the actual number of cycles of phase is unknown. These two estimates can be combined to obtain a more accurate $STEC$.

Once the STEC is computed from the combination of equation 4 and 5 based on Seemala and Valladares [21] TEC calibration technique, VTEC is obtained by taking the projection from the slant to the vertical using the thin shell model at Ionospheric Piercing Point (IPP), following the technique given by Komjathy and Langley (1996)

$$VTEC = STEC\cos(X') \quad (6)$$

where X' is the angle between the zenith angle and the angle of the GPS satellite at the IPP. The ionospheric irregularity indexes used here are based on Rate of TEC (ROT**)**, which is calculated directly from the $VTEC$ data for each Pseudo-Random Noise (PRN of GPS satellite) within intervals of 30 s using the following equation [6],

$$ROT = \frac{VTEC_u - VTEC_{u-1}}{t_u - t_{u-1}} \quad (7)$$

where u is the index of time of the epoch and ROT is computed for each 30 s interval and converted to the units of TECU/min.

[30] suggested that an index for the rate of TEC change of ROTI can be determined from the standard deviation of ROT in five-minute interval and mathematically it is given by

$$\boldsymbol{ROTI} = \sqrt{(\boldsymbol{ROT^2}) + (\boldsymbol{ROT})^2} \quad (8)$$

ROTI is a good indicator of the existence of ionospheric irregularities and $\boldsymbol{ROTI \geq 0.4}$ indicates the occurrence of irregular ionopheric activities relevant to ionospheric scintillation [33]

To estimate the percentage of ionospheric occurrence, if the $ROTI$ along the ray paths to any of the visible GPS satellites meet the aforementioned conditions, it is counted as one irregularity event and the percentage occurrence of irregularity is given by [32] $\frac{N(ROTI \geq threshold)}{N_{tot}} \times 100\%$, where N_{tot} number of total events.

2. DATA AND METHOD OF DATA ANALYSIS

The data used in this work were obtained from the Nigerian permanent GNSS Network (NIGNET, www.nignet.net), for the period of 2011- 2016. MATLAB and GOPI GPS-TEC analysis application software version 2.9.2 was used in the analysis of TEC data in this research work. The raw GPS data at 30 second sampling rate using GPS-TEC software (GOPI software - developed by Gopi Krishina Samela) to extract VTEC), time, azimuth and elevation angles, latitudes and longitudes from the raw GPS data. To eliminate multipath effects an elevation cut-off mark of $45°$ was used. The methods used to develop the GOPI software were illustrated in [34].

The months in the year were grouped into four seasons: March Equinox (February, March,

April), June Solstice (May, June, July), September Equinox (August, September, October) and December Solstice (November, December, January). The percentage occurrences of ionospheric irregularities at various stations and throughout the year 2011 – 2016 were identified (each day, month & season) based on GNSS irregularity index ROTI ≥ 0.4.

3. RESULTS AND DISCUSSION

In Table 1, we show the elevation of each station and the number of days data were available for the station in the period under study. GEMB station is at highest elevation of 1348 m above sea level, while RSUT and ULAG are at the lowest elevation of 46.6 m and 45.5 m respectively. BKFP with 1597 days of data, has the highest days of data available, while GEMB with 154 days of data has the lowest.

Fig. 2 illustrates specific occurrence of ionospheric irregularities at the various stations on daily basis during year 2011 - 2016. Note that the red colors represent instances and locations of occurrence of irregularities, the blue colors represent non-occurrence of irregularities, and the white spaces represent days with no available data. The criteria used to determine the occurrence of irregularity for a given day and station is that the values of ROTI ≥ 0.4 after local sunset for the day. There were lots of data gap during the study period due to the instrument breakdown. Despite this, we believe that the amount of data that we have is adequate for this study.

Fig. 2 shows that irregularities typically occur during the months of the year. It was found that the irregularities typically occurred during the equinoxes, where Feb until April is March equinox and August until October is September equinox. The analysis of Fig. 2 shows that irregularities rarely occur during the months of Dec - Jan and May - July which are solstice months, Nov - Jan is December solstice while May - July is the June solstice. It is already known that the TEC variations are greater during the equinoxes than during the solstices in the equatorial region [35,36] and the occurrence of irregularities is known to be more frequent during seasons of the year when TEC magnitudes are higher [32].

“For stations, as in the present study, which are located near the geographical equator, it is preferable to speak of the of the seasons in terms of solstices and equinoxes rather than the summer solstice, winter solstice, autumn equinox and spring equinox, the tropics do not experience significant levels of variations in the sun's intensity between the winter and the summer solstice and between the equinoxes like in the temperate region/polar regions, where remarkable differences are noticeable between the solstices (when the sun is away from the equator, on either side of it) and the equinoxes (when the sun is overhead the equator). During the June solstice, the sun is overhead the northern hemisphere, while during the December solstice, the sun is overhead the southern hemisphere. The sun is overhead the equatorial region during the equinoxes, this is why the TEC is usually greater at the equatorial region during the equinoxes. This explains why the frequency of occurrence of ionospheric irregularities and the magnitude are greater during equinoxes than during solstices in the equatorial region” [35,36].

The findings shows that the frequency of irregularity occurrence is highest in 2014 (which has more intensity of red colors relative to the blue colors compared to the other years that data were available). The reason for this is that the solar activity was greater in 2014 than in the other years, therefore the variation is connected to the solar activity. Solar activity are long-term variations which can be seen on year-to-year basis. This is because of the obvious reason that it takes a long term (~11 years) for a complete solar activity cycle to occur. Year 2011 was at the beginning of the rise of the solar cycle 24 (which from started from December 2008 and ended in December 2019, and it reached its peak in April 2014 – [37]) during which the solar activity level was slightly higher [38]. The TEC magnitudes are usually greater during years of higher solar activity than years of low solar activity, and this explains why the frequency of ionospheric irregularity occurrence and the magnitude were greater during high solar activity year (e.g. 2014) than during low solar activity years.

Fig. 2 also support the following observations: the highest occurrence of ROTI ≥ 0.4 were observed in April followed by March and May. “It implies that the highest occurrence of ionospheric irregularities occurs during the months of April, March, May and other months show relatively low ionospheric irregularities. This result is similar to the ionospheric scintillation occurrence reported” by [39,35]. Ionospheric irregularities occurrence at Nigeria

stations also show a seasonal trend. Irregularities were observed to be low around June/July but high during the months of March and September (see Tables 2-7).

"From the analysis of the time of occurrence, we note that ionospheric irregularity happens mostly at the post-sunset time, this is due to the eastward pre-reversal enhancement (PRE) electric field , which is coupled with the Earth's geomagnetic field to produce an upward vertical force derived from $\boldsymbol{E} \times \boldsymbol{B}$ (the curl of electric and magnetic field). The upward vertical force derived

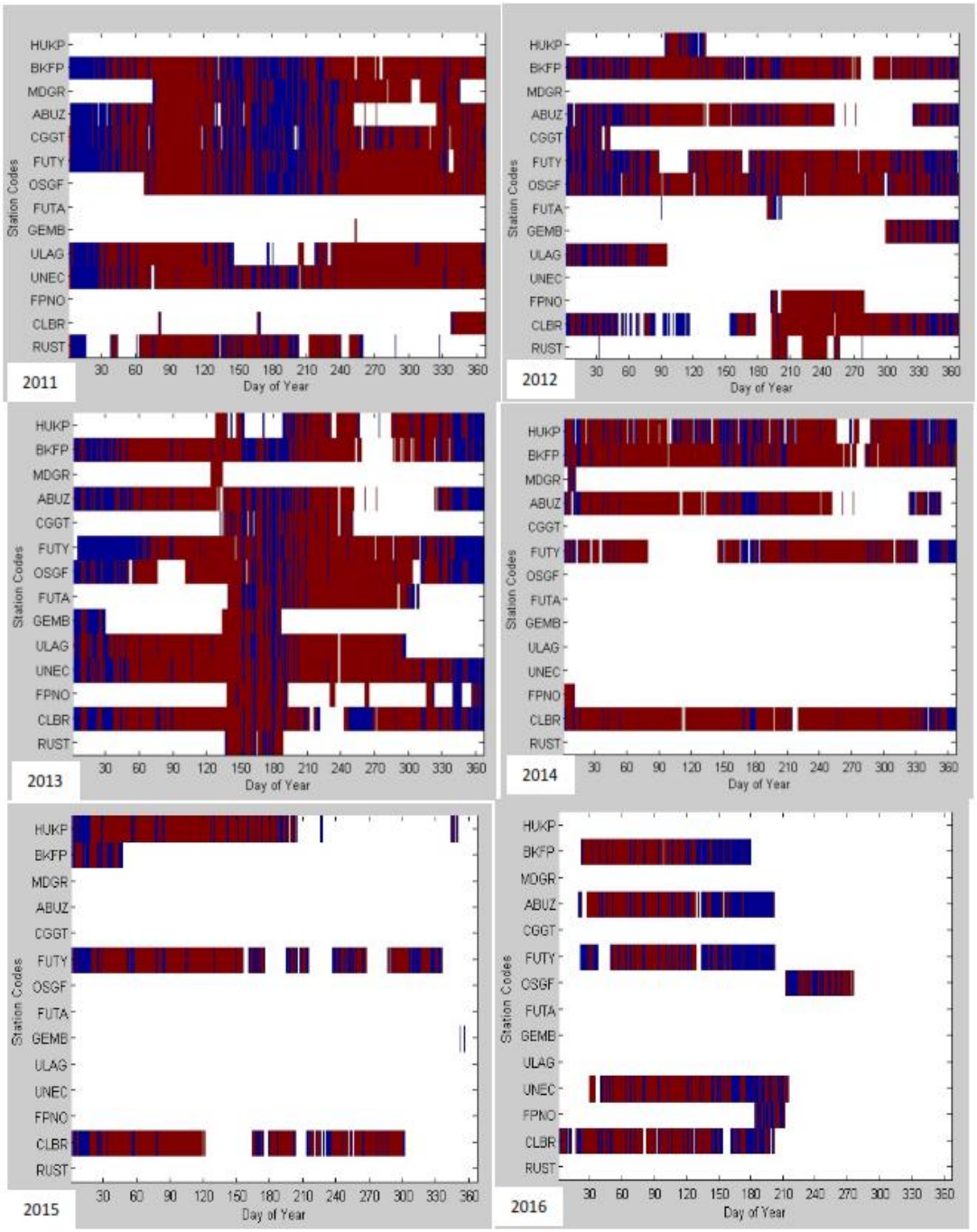

Fig. 2. Occurrence of ionospheric irregularity at the Nigerian stations during the days of year 2011-2016. The red colors represent instances and locations of occurrence of irregularities, the blue colors represent non-occurrence of irregularities, and the white spaces represent days with no available data

Table 2. Percentage occurrence of ionospheric irregularities for all the stations for the year 2011 with yearly average (Last 2 Columns) and monthly average of all the stations (Last 2 Rows)

2011	Feb	Mar	Apr	May	Jun	Jul	Aug	Sep	Oct	Nov	Dec	Jan	median	mean
ABUZ	50	88	98	55	38	28	60	99		88	92	8	60.0	64.0 ± 26.4
BKFP	60	93	98	48	42	45	72	99	99	85	95	15	78.5	70.9 ± 24.1
CGGT	60	90	99	60	80	85	70	100	100	90	88	12	86.5	77.8 ± 18.2
CLBR		100			99						99		99.0	99.3 ± 0.4
FPNO														
FUTA														
FUTY	50	82	98	60	58	31	75	99	100	85	85	10	78.5	69.4 ± 23.0
GEMB								100					100.0	100.0 ± 0.0
HUKP														
MDGR		92	88	55	50	25	50	95	100	88	100		88.0	74.3 ± 23.4
OSGF		100	100	60	35	30	70	100	100	95	90		92.5	78.0 ± 23.4
RUST	79	99	98	70	75	75	90	99				15	79.0	77.8 ± 16.9
ULAG	78	98	98	60		100	83	100	100	85	98	22	98.0	83.8 ± 16.8
UNEC	65	95	95	65	55	57	90	100	100	90	92	15	90.0	76.6 ± 21.0
Median	60.0	93.0	98.0	60.0	54.0	38.0	71.0	99.0	100.0	88.0	93.5	13.5		
Mean	62.8	93.6	97.1	58.5	59.6	52.4	71.3	99.0	99.8	88.0	93.4	13.7		

Table 3. Percentage occurrence of ionospheric irregularities for all the stations for the year 2012 with yearly average (Last 2 Columns) and monthly average of all the stations (Last 2 Rows)

2012	Feb	Mar	Apr	May	Jun	Jul	Aug	Sep	Oct	Nov	Dec	Jan	median	mean
ABUZ	38	80	98	97	62	69	90	88		62	50	45	69.0	70.8 ± 18.0
BKFP	72	90	98	75	49	75	98	85	95	84	50	49	79.5	76.7 ± 15.0
CGGT	70											55	62.5	62.5 ± 7.5
CLBR	68	100			99	91	100	100	92	70	40	49	91.5	80.9 ± 19.3
FPNO						90	100	98	100				99.0	97.0 ± 3.5
FUTA						100							100.0	100.0 ± 0.0
FUTY	35	68	82	89	78	80	95	95	85	50	30	41	79.0	69.0 ± 20.2
GEMB									78	79	50		78.0	69.0 ± 12.7
HUKP		88	100										94.0	94.0 ± 6.0
MDGR														
OSGF	45	75	98	85	75	75	95	98	90	80	45	48	77.5	75.8 ± 15.3
RUST						95	100	82					95.0	92.3 ± 6.9
ULAG	68	90	95									46	79.0	74.8 ± 17.8
UNEC														
Median	68	88	98	87	75	85	98	95	91	74.5	47.5	48	86.0	
Mean	56.6	84.4	95.2	86.5	72.6	84.4	96.9	92.3	90.0	70.8	44.2	47.6	84.4	

Table 4. Percentage occurrence of ionospheric irregularities for all the stations for the year 2013 with yearly average (Last 2 Columns) and monthly average of all the stations (Last 2 Rows)

2013	Feb	Mar	Apr	May	Jun	Jul	Aug	Sep	Oct	Nov	Dec	Jan	median	mean
ABUZ	50	89	94	88	42	40	82	87		70	10	29	70.0	61.9 ± 25.2
BKFP	68	98	99	90	30	55	98	99	99	80	28	29	85.0	72.8 ± 25.6
CGGT				89	69	75	90	100					89.0	84.6 ± 10.1
CLBR	75	80	100	100	81	82	100	100	98	87	38	30	84.5	80.9 ± 16.8
FPNO				99	85	80	100	100		80	30		85.0	82.0 ± 16.0
FUTA				92	50	70	100	100	100	100			100.0	87.4 ± 15.7
FUTY	8	70	98	95	69	60	99	100	95	60	20	4	69.5	64.8 ± 28.7
GEMB					99	72	72					20	72.0	65.8 ± 22.9
HUKP				90		58	95	99	88	85	30		88.0	77.9 ± 19.3
MDGR				100									100.0	100.0 ± 0.0
OSGF	52	100	98	100	62	70	98	100	98	80	15	25	89.0	74.8 ± 25.0
RUST				100	70	100							100.0	90.0 ± 13.3
ULAG	78	98	98	98	60	100	100	100	96			51	98.0	87.9 ± 14.9
UNEC	68	95	98	100	75	96	98	100	98	86	25	55	95.5	82.8 ± 18.1
Median	60	93.5	98	96.5	69	71	98	100	98	80	28	29	86.8	
Mean	55.2	89.2	97.8	95.1	65.2	71.8	94.0	98.5	96.3	80.3	24.4	26.9	84.7	

Table 5. Percentage occurrence of ionospheric irregularities for all the stations for the year 2014 with yearly average (Last 2 Columns) and monthly average of all the stations (Last 2 Rows)

2014	Feb	Mar	Apr	May	Jun	Jul	Aug	Sep	Oct	Nov	Dec	Jan	median	mean
ABUZ	90	99	99	95	48	85	99	99		70	44	78	90.0	82.4 ± 16.3
BKFP	93	100	100	90	58	72	100	100	98	75	64	78	91.5	85.7 ± 13.6
CGGT														
CLBR	89	100	100	100	79	98	100	98	98	90	40	90	98.0	90.2 ± 10.5
FPNO												90	90.0	90.0 ± 0.0
FUTA														
FUTY	88	100		84	85	89	99	100	92	65	22	83	88.0	82.5 ± 14.2
GEMB														
HUKP	90	100	100	100	55	78	98	100	97	76	45	88	93.5	85.6 ± 14.7
MDGR												50	50.0	50.0 ± 0.0
OSGF														
RUST														
ULAG														
UNEC														
Median	90	100	100	95	58	85	99	100	97.5	75	44	83	92.5	
Mean	90.0	99.8	99.8	93.8	65.0	84.4	99.2	99.4	96.3	75.2	43.0	79.6	91.9	

Table 6. Percentage occurrence of ionospheric irregularities for all the stations for the year 2015 with yearly average (Last 2 Columns) and monthly average of all the stations (Last 2 Rows)

2015	Feb	Mar	Apr	May	Jun	Jul	Aug	Sep	Oct	Nov	Dec	Jan	median	mean
ABUZ														
BKFP	41											61	51.0	51.0 ± 10.0
CGGT														
CLBR	89	98	100		70	88	80	91	90			49	89.0	83.9 ± 11.7
FPNO														
FUTA														
FUTY	89	93	98	93	55	45	32	64	95	45		40	64.0	68.1 ± 23.2
GEMB														
HUKP	95	90	100	88	86	65				65		45	87.0	79.3 ± 15.7
MDGR														
OSGF														
RUST														
ULAG														
UNEC														
Median	89	93	100	90.5	70	65	56	78	92.5	55		47	77.5	
Mean	78.5	93.7	99.3	90.5	70.3	66.0	56.0	77.5	92.5	55.0		48.8	77.5	

Table 7. Percentage occurrence of ionospheric irregularities for all the stations for the year 2016 with yearly average (Last 2 Columns) and monthly average of all the stations (Last 2 Rows)

2016	Feb	Mar	Apr	May	Jun	Jul	Aug	Sep	Oct	Nov	Dec	Jan	median	mean
ABUZ	88	78	69	39	18	8						78	69.0	54.0 ± 27.7
BKFP	90	88	71	35	19							81	76.0	64.0 ± 24.7
CGGT														
CLBR	78	90	89	78	48	62						68	78.0	73.3 ± 12.0
FPNO						60							60.0	60.0 ± 0.0
FUTA														
FUTY	60	80	72	50	30	15						25	50.0	47.4 ± 20.7
GEMB														
HUKP														
MDGR														
OSGF						100	39	75					75.0	71.3 ± 21.6
RUST														
ULAG														
UNEC	100	80	78	88	68	40	50						78.0	72.0 ± 16.6
Median	88	80	72	50	30	50	44.5	75				73	72.0	
Mean	83.2	83.2	75.8	58.0	36.6	47.5	44.5	75.0				63.0	63.0	

from gradient of ion and electron densities between the upper and lower layer, thereby producing plasma bubble irregularities, arising from Rayleigh-Taylor instability process" [40]. Fig. 2 also shows that "occurrence of ionospheric plasma irregularities are the highest throughout the month of April. The result also matched result reported" by [41]. "The explanation for the high ionospheric irregularity occurrence in April is that April is an equinoctial month" [42].

3.1 Percentage Occurrence of Ionospheric Irregularity

To determine whether or not an irregularity occurred at a particular station during a particular day, the ROTI values after local sunset (18:00 LT) are examined. The criterion for occurrence of irregularity is that ROTI $\geq$ 0.4. The days with post-sunset ROTI $\geq$ 0.4 are flagged as 1 to denote occurrence of irregularity, the days with ROTI $\leq$ 0.4 are flagged as 0 to denote non-occurrence of irregularity, and the days with no available data are flagged as NaN. The percentage occurrence of irregularity for a given month is computed by dividing the number of days flagged as 1 in that month by the total number of days flagged as 0 and 1 in that month, times 100%. The days with no available post-sunset data were not included in the total number of days because no decision is taken about such days regarding whether or not irregularities occurred in them.

In Table 2, at ABUZ station in 2011, the recorded percentage ionospheric irregularities during March Equinox were around 50%, 88% and 98% respectively. During June Solstice, our results show that the recorded percentage occurrence of ionospheric irregularity were around 55%, 38% and 28% respectively. In September Equinox the percentage of occurrence of ionospheric irregularity according to our result stood around 60%, 99% for the months of August and September respectively, October records were not available. For December Solstice, our result indicates that the percentage occurrence of ionospheric irregularity stood around 88%, 92% & 45%.

Our results for ABUZ station in 2012 are as follows: in March Equinox, the percentage occurrence of ionospheric irregularity stood around 38%, 80% and 98%; during June Solstice, the percentage occurrence of ionospheric irregularity recorded were around 97%, 62% and 69%; in September Equinox, we have the percentage occurrence of ionospheric irregularity around 90% & 88% . In December Solstice (including January 2013), the percentage occurrences of ionospheric irregularity recorded around 62%, 50% & 45%.

Our result also indicated that the percentage occurrences of ionospheric irregularity recorded at ABUZ station in 2013 were as follows: March Equinox - 50%, 89% and 94%; June Solstice - 88%, 42% and 40%; September Equinox - 82% & 87%; December Solstice (including January 2014) - 70%, 10% & 29%.

Our result also indicated that the percentage occurrences of ionospheric irregularity recorded at ABUZ station in 2014 were as follows: March Equinox - 90%, 99% and 99%; June Solstice - 95%, 48% and 85%; September Equinox - 99% & 99% . December Solstice - 70% & 44%. There were no records for the year 2015. Our results for the year 2016 indicated that the percentage occurrences of ionospheric irregularities at ABUZ station were as follows; March Equinox - 88%, 78% and 69%; June Solstice - 39%, 18% and 8%. Records were unavailable for the remaining months of 2016. All other stations showed similar trends, and the results were displayed in Tables 2 – 7.

The highest value of percentage occurrence of ionospheric irregularities were around March Equinox and September Equinox. The result also matched with the result reported by [41]. The explanation for the high ionospheric irregularity occurrence in April is that April is an equinoctial month in which the magnetic meridian is closely aligned with the solar terminator [42,43]. This is evident in Table 8, where we used the monthly average (median and mean) for all the stations and for year 2011-2016, the months of April and October have the highest percentage occurrences of ionospheric irregularities. Using the monthly median values, the percentage occurrence of ionospheric irregularities for the month of April is 98.0% (median) and $94.3 \pm 7.4\%$ (mean), while that of the month of October is 98.0% (median) and $94.1 \pm 3.3\%$ (mean); while using the monthly mean values, the percentage occurrence of ionospheric irregularities for the month of April is 97.5 (median) and $94.2 \pm 6.1\%$ (mean) while that of October is 96.3 (median) and 94.0 ± 3.0 (mean).

Table 8. Monthly average percentage occurrence of ionospheric irregularities for the year 2011-2016 for all stations all taken together (using the monthly median and the mean values for all the stations)

Using median value of the monthly average for each year												
Year	**Feb**	**Mar**	**Apr**	**May**	**Jun**	**Jul**	**Aug**	**Sep**	**Oct**	**Nov**	**Dec**	**Jan**
2011	60	93	98	60	54	38	71	99	95	88	94	14
2012	68	88	98	87	75	85	98	95	91	75	48	48
2013	60	94	98	97	69	71	98	100	98	80	28	29
2014	90	100	100	95	58	85	99	100	98	75	44	83
2015	89	93	100	91	70	65	56	76	92	55		47
2016	88	80	72	50	30	50	45	75				73
median	78.0	93.0	98.0	89.0	64.0	68.0	45.0	97.0	98.0	75.0	46.0	48.0
mean	75.8± 13.2	91.25±4.8	94.3± 7.4	79.8±16.6	59.3±12.0	65.7±14.7	77.8±20.6	91.1±9.8	94.1±3.30	74.5±7.8	53.3±20.1	48.9±19.4
Using mean value of the monthly average for each year												
Year	**Feb**	**Mar**	**Apr**	**May**	**Jun**	**Jul**	**Aug**	**Sep**	**Oct**	**Nov**	**Dec**	**Jan**
2011	62.8	93.6	97.1	58.5	59.6	52.4	71.3	99.0	99.8	88.0	93.4	13.7
2012	56.6	84.4	95.2	86.5	72.6	84.4	96.9	92.3	90.0	70.8	44.2	47.6
2013	55.2	89.2	97.8	95.1	65.2	71.8	94.0	98.5	96.3	80.3	24.4	26.9
2014	90.0	99.8	99.8	93.8	65.0	84.4	99.2	99.4	96.3	75.2	43.0	79.6
2015	78.5	93.7	99.3	90.5	70.3	66.0	56.0	77.5	92.5	55.0		48.8
2016	83.2	83.2	75.8	58.0	36.6	47.5	44.5	75.0				63.0
median	70.7	91.4	97.5	88.5	65.1	68.9	82.6	95.4	96.3	75.2	43.6	48.2
mean	71.0± 12.9	90.6±5.0	94.2± 6.1	80.4± 14.8	61.6± 9.0	67.7±12.5	77.0±19.7	90.3± 9.4	95.0± 3.0	73.9± 8.8	51.2±21.1	46.6±17.5

We also calculated the averaged percentage occurrence of ionospheric irregularities using the median values from all the station and for all the years under study, and the values for March and September equinoxes are higher than June and December solstices. Generally, the results indicate that during September equinox, occurrence of ionospheric irregularities is highest and the lowest occurrence is during December Solstice.

The two peaks of irregularity seasons were observed at all the stations for the year 2011-2016. The peaks occur around the equinoxes. Ionospheric irregularities responsible for GPS scintillations at low latitude are primarily associated with equatorial spread in F region [2]. Many other authors found the maximum occurrence of ionospheric scintillation during Equinox months [44,45].

Dividing the stations into geographical north (ABUZ, BKFP, CGGT, FUTY, GEMB, HUKP, MDGR and OSGF) and south (CLBR, FPNO, FUTA, RUST, UNEC and ULAG) of Nigeria, the result indicates that ionospheric irregularities occur more in the southern than in the northern geographical locations in Nigeria. The calculated average values using the monthly median values are: 78.55 ± 10.88% for the stations based in northern Nigeria and 89.83 ± 8.21% for the stations based in southern Nigeria respectively; while using the monthly mean values, we have 72.82±9.65% for the stations based in northern Nigeria and 83.95±7.45% for the stations based in southern Nigeria respectively.

The average result we obtained the March Equinox (February, March April) months for the all the years under study is 82.40±15.89%, June Solstice (May, June, July) months is 64.05 ± 15.89%, September Equinox (August, September, October) months is 89.94±11.01% and for December Solstice (November, December, January) is 56.81 ± 23.62% for stations based in northern geographical zone of Nigeria, while for stations based in southern geographical zone we have - March Equinox - 89.08±9.68%; June Solstice - 80.64±14.83%; September Equinox - 95.43±5.99%; December Solstice - 61.79±25.72%.

These results are indications that the occurrences of ionospheric irregularities are greater during equinoxes than during solstices and there are higher percentages of ionospheric irregularities to occur in the southern Nigeria than northern Nigeria. This differences in percentage occurrence of ionospheric irregularities between the geographical north and south of Nigeria might be attributed to differences in their geographical and geomagnetic longitude and latitude. The average geographical and geomagnetic longitude and latitude are: geographical longitude and latitude - 9.18±2.47 and 10.47±1.62 - and geomagnetic longitude and latitude -81.03±2.07 and -0.89±0.94 - for northern stations while for southern station, the average geographical and geomagnetic longitude and latitude are: geographical longitude and latitude - 6.40±1.4 and 5.90±0.84 - and geomagnetic longitude and latitude - 76.95±2.53 and -3.56±.61. There are noticeable differences especially in both geographic and geomagnetic latitude.

The occurrences of ionospheric irregularities were observed to increase with solar activity. The average percentage ionospheric irregularities calculated using the using the monthly averages for the whole stations for the years were: 2011 - 2016 (in %): 73.05, 78.22, 75.67, 85.52, 75.53 and 62.77, respectively. This result shows that ionospheric irregularities in Nigeria for the year 2011-2016 started to increase from 2011, reached its peak in 2014 and started to wane from 2015. This observed trend closely follow sunspot number trend for solar cycle 24 which began in 2008, reached its maximum in 2014 [46].

4. CONCLUSION

In this study, we have carried an investigation of ionospheric irregularities over Nigeria, an equatorial region using global navigation satellite system. We have used 5-min ROTI and 30-s ROT from 30-s RINEX data to study the occurrence of ionospheric irregularities over large-scale ionospheric irregularities over Nigerian stations. The data covered a period of six years, i.e., 2011 - 2016 at 14 stations.

Our result revealed significant latitudinal differences, we observed consistent occurrence of irregularities across all the stations, with particularly strong and consistent occurrence at the CLBR station in Calabar, Nigeria. The station is located farther from the geomagnetic equator and closer to the southern anomaly crest, exhibited a higher occurrence of irregularities. It is clearer that TEC variability is greatly influenced by the geographical location of the Earth's magnetic field, while the patterns of variability are modulated by the Earth's diurnal rotation.

Our results exhibited a level uniformity with the previous studies that have used different methods and indices to study the ionospheric irregularities over an equatorial region, Nigeria. We summaries our findings below.

- This study reveal difference in the strength of ionospheric irregularities over stations located within the same equatorial region in Nigeria. This was attributed to the difference in the geomagnetic latitudes of the stations.
- The variability of TEC is greatly influenced by the geographical location of Earth's magnetic field, while its spatial patterns of variability are modulated by the Earth's diurnal rotation [47]. At equatorial stations located on the north side of the magnetic equator, there is a significant depletion of TEC. These variations affects the accuracy of satellite-based communication and navigation systems [48].
- Seasonal equatorial TEC irregularities (as shown in high values of ROTI) were observed during 2014. It exhibited a bimodal feature showing equinoctial asymmetry in the strength of ionospheric TEC irregularities confirm observations from earlier studies in other (near) equatorial regions in Africa [e.g., 49].
- The seasonal TEC irregularities were characterized by stronger TEC irregularities in the March equinox and September equinox season. The reduction of ROTI and ROT during the September equinox could be attributed to the suppressing role of the dynamo electric field. This requires further investigation.
- The percentage occurrences of ionospheric irregularities vary throughout the period, March and September equinoxes has the highest occurrence of ionospheric irregularity. We also observed that ionospheric irregularities mostly occur during the night- time in the March equinox and September solstice in the year 2014 because of high solar activity.

Conclusively, we found out that ionospheric irregularities which are disturbances in the ionosphere which can affect propagation of radio waves between space and ground-based systems, by disrupting the transmission of satellite-based radio communication signals, and sometimes cause blackouts of the signals for satellite navigation systems like Global Positioning System (GPS). These irregularities ionospheric can occur randomly, but increased in frequency of occurrence during the months of equinoxes and follow solar cycle in the frequency and magnitude of occurrence. Interestingly, these satellite navigation systems have provided avenue to investigate the structure of the ionosphere and the associated ionospheric irregularities in the ionosphere. We could also conclude that ionospheric irregularities occur more in equator-ward region than at the magnetic equatorial and the poleward EIA regions.

In estimating the magnitude of ionospheric irregularities using ROTI, there were some drawbacks/limitations and advantages in ROTI calculation. The ROTI index does not contain information about the scale size or frequency of irregularities, only that irregularity exists within the range limited by the sample rate and measurement interval. Assuming that the density irregularities do not change within a short time as they pass the receiver-to-satellite line-of-sight, the irregularities may be converted to spatial gradient of TEC [9,30,50]. One advantage of using ROTI to estimate ionospheric irregularities is that, the calculation of ROTI is quite straightforward, can be calculated based on data from normal GNSS receivers, there is a lot of data available, with global coverage, though the equations for ROTI uses the rate-of-change of the geometry-free combination, the biases and ambiguities that often complicate analysis of GNSS data are eliminated.

ACKNOWLEDGEMENTS

We want acknowledged the entire staff of CAR-NARSDA to Abuja, especially Dr. D. Okoh for giving access to almost all their facilities, while carrying out this work. We also acknowledged Nigerian Permanent GNSS Network (NIGNETS) and CAR-NARSDA Abuja for assembling and maintaining the GPS Data base, which is the basis of this study.

COMPETING INTERESTS

Authors have declared that no competing interests exist.

REFERENCES

1. Wanniger L. Effects of the Equatorial Ionosphere on GPS. GPS World. 1993; 4(7): 48-53.

2. Kintner PM, Ledvina BM, de Paula ER. GPS and Ionospheric scintillations Space Weather . 2007;5:S09003.
DOI: 10.1029/2006SW000260
3. Oladipo OA, Schuler T. Equatorial ionospheric irregularities using GPS TEC derived index. J. Atmos. Solar-Terrestrial Phys. 2013a ;92:78-82.
DOI: 10.1016/j.jastp.2012.09.019
4. Abdu MA, Medeiros RT, Bittencourt JA, Batista IS. Vertical ionization drift velocities and range type spread F in the evening equatorial ionosphere. J. Geophys. Res. 1983;88:399-402.
DOI: 10.1029/JA088iA01p00399
5. Kil H, Heelis RA, Paxton LJ, Oh SJ. Formation of a plasma depletion shell in the equatorial ionosphere. J. Geophys. Res. Space Phys. 2009;114(A11):A11302.
DOI: 10.1029/2009JA014369
6. Basu S, Groves KM, Quinn JM, Doherty P. A comparison of TEC fluctuations and scintillations at Ascension Island. J. Atmos. Solar-Terrestrial Phys. 1999;61(15):1219-1226.
DOI: 10.1016/s1364-6826(99)00052-8
7. Alfonsi L, Spogli L, Pezzopane M, Romano V, Zuccheretti E, de Franceschi G, et al. Comparative analysis of spread-F signature and GPS scintillation occurrences at Tucumán, Argentina Journal of Geophysical Research: Space Physics. 2013;118(7):4483-4502.
DOI: 10.1002/jgra.50378
8. Liu K, Li G. Ning L, Hu, Li H. Statistical characteristics of low-latitude ionospheric Scintillation over China, Adv. Sp. Res. 2015;55(5):1356- 1365.
9. Jacobsen KS. The impact of different sampling rates and calculation time intervals on ROTI values, J. Sp. Weather Sp. Clim. 2014;4(A33):1-9.
10. Davies K. Ionospheric Radio Peter Peregriuns Ltd, London; 1990.
11. McNamara LF, Wilkinson OJ. Prediction of Total Electron content using the International Reference Ionosphere. Journal of Atmosphere and Terrestrial Physics. 1991;45(2/3):164.
12. Rastogi RG. Seasonal variation of equatorial spread F in the American and Indian zones. J. Geophys. Res. Space Phys. 1980;85(A2):722-726.
DOI: 10.1029/JA085iA02p00722
13. Fejer BG, Scherliess L, de Paula ER. Effects of the vertical plasma drift velocity on the generation and evolution of equatorial spread F. J. Geophys. Res. 1999;104:19859-19869.
DOI: 10.1029/1999ja900271
14. Oladipo OA, Schuler T. Magnetic storm effect on the occurrence of ionospheric irregularities on an equatorial station in the African sector. Ann. Geophys. 2013b; 56(5):A0565.
DOI: 10.4401/ag-6397
15. Sharma AK, Chavan GA, Gaikwad HP, Gurav OB, Nade DP, Nikte SS, et al. Study of ionospheric irregularities from Kolhapur. J. Atmos. Solar-Terrestrial Phys. 2018;173:16-22.
DOI: 10.1016/j.jastp.2017.12.019
16. Bolaji OS, Adebiyi SJ, Fashae J, Ikubanni SO, Adenle HA, Owolabi C. Pattern of latitudinal distribution of Ionospheric Irregularities in the African region and the effect of March 2015 St. Patrick's Day storm. J. Geophys. Res. Space Phys. 2020;125:e2019JA027641.
DOI: 10.1029JA027641
17. De Rezende LFC, De Paula ER, Batista IS, Kantor IJ, De Assis Honorato, Muella MT. Study of ionospheric irregularities during intense magnetic storms. Braz. J. Geophys. 2007;25:151-158.
DOI: 10.1590/s0102-261x2007000600017
18. Sobral JHA, Abdu MA, Takahashi H, Taylor MJ, de Paula ER, Zamlutti CJ, et al. Ionospheric plasma bubble climatology over Brazil based on 22 years (1977-1998) of airglow observations. J. Atmos. Solar-Terrestrial Phys. 2002;64:1517-1524.
DOI: 10.1016/s1364-6826(02)00089-5
19. Chu FD, Liu JY, Takahashi H, Sobral JHA, Taylor MJ, Medeiros AF. The climatology of ionospheric plasma bubbles and irregularities over Brazil. Ann. Geophys. 2005;23:379-384.
DOI: 10.5194/angeo-23-379-2005
20. Muella MTAH, de Paula ER, Kantor IJ, Batista IS, Sobral JHA, Abdu MA, et al. GPS L-band scintillations and ionospheric irregularity zonal drifts inferred at equatorial and low-latitude regions. J. Atmos. Solar-Terrestrial Phys. 2008;70: 1261–1272.
DOI: 10.1016/j.jastp.2008.03.013
21. Seemala G, Valladares CE. Statistics of total electron content depletions observed over the South American continent for the year 2008. Radio Sci. 2011;46:1.
DOI: 10.1029/2011RS004722
22. Ngwira CM, Seemala GK, Habarulema JB. Simultaneous observations of ionospheric

irregularities in the African low-latitude region. J. Atmos. Solar-Terrestrial Phys. 2013;97:50-57.
DOI: 10.1016/j.jastp.2013.02.014

23. Mungufeni P, Habarulema JB, Jurua E. Trends of ionospheric irregularities over African low latitude region during quiet geomagnetic conditions. J. Atmos. Solar-Terrestrial Phys. 2016;138-139:261-267.
DOI: 10.1016/j.jastp.2016.01.015
24. Okoh D, Rabiu B, Shiokawa K, Segun Y, Falayi E, Kaka R. First study on the occurrence frequency of equatorial plasma bubbles over West Africa of equatorial plasma bubbles over West Africa using an all-sky airglow imager and GNSS receivers. Journal Geophysical Research: Space Physics. 2017;122(12):430 -12,444.
Available:http://doi.org/10.1002/2017JA024602.
25. Amaechi PO, Oyeyemi EO, Akala AO. Geomagnetic storm effects on the occurrences of ionospheric irregularities over the African equatorial/low-latitude region. Adv. Space Res. 2018a;61(8):2074-2090.
DOI: 10.1016/j.asr.2018.01.035
26. Amaechi PO, Oyeyemi EO, Akala AO. The response of African equatorial/low-latitude ionosphere to 2015 St. Patrick's Day geomagnetic storm. Space Weather. 2018b;16:601-618.
DOI: 10.1029/2017sw001751
27. Bolaji OS, Adebiyi SJ, Fashae J, Ikubanni SO, Adenle HA, Owolabi C. Pattern of latitudinal distribution of Ionospheric Irregularities in the African region and the effect of March 2015 St. Patrick's Day storm. J. Geophys. Res. Space Phys. 2020;125:e2019JA027641.
DOI: 10.1029JA027641
28. Dugassa T, Habarulema JB, Nigussie M. Longitudinal variability of occurrence of ionospheric irregularities over the American, African and Indian regions during geomagnetic storms. Adv. Space Res. 2019;63(11):2609-2622.
DOI: 10.1016/j.asr.2019.01.001
29. Ikani O, Okeke FN, Okpala KC, Rabiu B. Diurnal and seasonal variation s of the occurrence of Ionospheric Irregularities over Nigeria from GNSS data. Front. Astron. Space Sci. 2023;10: 11255950.
DOI: 10.3389 f/spas. 2023.1125950
30. Pi X, Mannucci AJ, Lindqwister UJ, Ho CM. Monitoring of global ionospheric irregularities using the world-wide GPS network. Geophys. Res. Lett. 1997;24(18): 2283-2286.
DOI: 10.1029/97GL02273
31. Okoh D, Owolabi O, Ekechukwu C, Folarin O, Arhiwo G, Agbo J, et al. A regional GNSS-VTEC model over Nigeria using neural networks: A novel approach Geodesy and Geodynamics. 2016;7(1): 19e31.
Available:http://dx.doi.org/10.1016/j.geog.2016.03.003
32. Mulugeta S, Kassa T. Nighttime ionospheric irregularities inferred from rate of total Electron Content Index (ROTI) values over Bahir Dar, Ethiopia, Advances in Space Research; 2020.
DOI:
https://doi.org/10.1016/j.asr.2020.11.030
33. Yang Z, Liu Z. Correlation between ROTI and Ionospheric Scintillation Indices using Hong Kong low- latitude GPS Dat. GPS Solut. 2015;2015(20):815-824.
34. Rao PVS, Gopi KS, Niranjan K, Prasad SVD. Temporal and spatial variations in TEC using simultaneous measurements from the Indian network of receivers during the low solar activity period of 2004-2005. Ann Geophys. 2006;24:3279-3292.
35. Okoh D, Ambrose E, Okere B, McKinnell LA, Okeke PN. Does IRI really know Nsukka. A comparison of IRI- TEC with GPS-TEC over Nsukka, Nigeria. Paper presented at IRI 2012 Workshop, SANSA Space Sci, Hermanus South Africa; 10-14 Oct 2012.
36. Okonkwo CP, Ugwuanyi M. 'IRI and GPS TEC Variations over Ilorin, Nigeria. Journal of space science \& Technology. 2012;1:Index 3.
37. Available:www.sidc.be
38. Olwendo J, Cilliers PJ, Ming N. Monthly trends in temporal and spatial distribution of Ionospheric Irregularities across the African region during the descending phase of solar cycle 24. Advances in Space Research. 2021;67(2021):3187-3201.
39. Seba EB, Gogie TK. Investigating the effect of geomagnetic storm and equatorial electrojet on equatorial ionospheric irregularity over East African sector. Advances in Space Research. 2015;58(9): 1708-1719.
40. Kelly MC, Makela J, Ledvina M, Kinter PM. The Earth's Ionosphere Plasma physics

and Electrodynamics, 96, Second Ed eBook. Academics Press, Elsevier, New-York; 2009.
ISBN: 9780080916576.

41. Akala AO, Oluyo S. Comparison of equatorial GPS-TEC observations over an African station and American station during the minimum and ascending phases of solar cycle 24. Ann. Geophys. 2013, 2017;31:20852096.
42. Tsunoda RT. Control of the seasonal and longitudinal occurrence of equatorial scintillations by the longitudinal gradient in integrated E region Pedersen conductivity. J. Geophys. Res. 1985;90(A1):447-456.
DOI: 10.1029/JA090iA01p00447
43. Abdu MA, Medeiros RT, Bittencourt JA, Batista JS. Vertical ionization drift velocities and range type spread F in the evening equatorial Ionosphere. J. Geophys. Res. 2009;88:399-402.
DOI: 10.1029/JA088ip00399
44. Nishioka M, Saito A, Tsugawa T. Occurrence characteristics of plasma bubble derived from global ground-based GPS receiver networks. J. Geophys. Res. Space Phys. 2008;113:A05301.
DOI: 10.1029/2007JA012605
45. Thanh Heelis RA, Depew MD. Ionospheric Connections (ICON) Ion Velocity Meter (IVM) Observations of the Equatorial Ionosphere at Solar Minimum; 2021.
46. Available:www.SISLO.com
47. Calabia A, Jin S. New modes and mechanisms of long-termionospheric TEC variations from globalionosphere maps. J. Geophys. Res. Space Phys. 2020;125: e2019JA027703.
DOI: 10.1029/2019JA027703
48. Shah M, Abbas A, Ehsan M, Calabia A, Adhikari B, Tariq M, et al. Ionospheric thermospheric responses in South America to the August 2018 geomagnetic storm based on multiple observations. IEEE J. Sel. Top. Appl. Earth Observations Remote Sens. 2022;15:261-269.
DOI: 10.1109/JSTARS.2021.3134495
49. Olwendo OJ, Baluku T, Baki P, Cilliers PJ, Mito C, Doherty P. Low latitude ionospheric scintillation and zonal irregularity drifts observed with GPSSCINDA system and closely spaced VHF receivers in Kenya. Adv. Space Res. 2013;51:1715-1726.
DOI: 10.1016/j.asr.2012.12.017
50. Liu Z, Chen W. Study of the Ionospheric TEC Rate in Hong Kong Region and it's GPS/GNSS application Global Navigation Satellite System: Technology Innovation and Application. 2009;9778 - 1 - 935068-03-7.

Peer-review history:
The peer review history for this paper can be accessed here:
https://prh.globalpresshub.com/review-history/1475